

Parametric study of random fields of the mechanical properties of the material in a peridynamic model

Caroline Bremm¹, Mylena Barcellos da Silva¹, Leandro F Friedrich¹, Luis E Kosteski², Ignacio Iturrioz³

¹Dept. Mechanical Engineering, Universidade Federal do Pampa, Campus Alegrete. Av. Tiaraju 810, CEP 97546-550, RS/Alegrete, Brazil.

carolbremm98@gmail.com, mylenabsilva@gmail.com, leandrofriedrich@unipampa.edu.br

²Engineering Post-Graduate Program, Universidade Federal do Pampa, Campus Alegrete. Av. Tiaraju 810, CEP 97546-550, RS/Alegrete, Brazil.

luiskosteski@unipampa.edu.br

³Mechanical Post-Graduate Program, Universidade Federal do Rio Grande do Sul
Sarmiento Leite 425, CEP 90050-170, RS/Porto Alegre, Brazil.

ignacio.iturrioz@ufrgs.br

Abstract. Simulations based on the peridynamic theory are a promising approach to understand the processes involved in the fracture of different materials. Failure mechanisms of materials are intrinsically related with nonhomogeneity and randomness on small scales. This fact is an important aspect, because it can change the mechanical behavior and the fracture location. This work presents a parametric study of the implementation of the material's specific fracture energy (G_f) correlated random fields. The specific fracture energy, which is directly related to the critical stretching of peridynamic bonds, is defined as a 3D scalar random field with Weibull probability distribution and a defined correlation length. A plate subjected to a traction load illustrates the proposed approach. The results shows an independence of the fracture pattern with the level of discretization used. This parametric study contribute to provide flexibility in the calibration of the peridynamic model response allowing that the fracture patterns and the global material behavior to change and mainly disconnected from discretization.

Keywords: Peridynamics, random field, specific fracture energy.

1 Introduction

Heterogeneous materials in a more general sense are those that are formed by domains of different materials (phases) or the same material, but in different states. In the first case, composite materials in general can be cited as materials reinforced with fibers and particles, copolymers, foams, concrete, among others. In the second, it is possible to highlight the polycrystals, soils, wood, bone, sea ice and others. These examples show that most of the materials we know are heterogeneous and are not only part of the engineering materials (chemistry, mechanics, civil, aerospace) but are overlapped with other areas such as physics, geophysics, biology, among others which makes research on these materials a multidisciplinary topic [1]. For modeling heterogeneous materials, it becomes computationally expensive to represent in a model all the heterogeneities (phases) of a material such as pores and inclusions, for example. An alternative is then to use the random field models where a class of material is represented by sharing some average characteristics of the material such as density, porosity, stiffness, etc. [2].

This work presents a parametric study of the implementation of correlated random fields of the specific fracture energy of the material, G_f , in the peridynamic (PD) model. PD is a reformulation of non-local continuous mechanics capable of incorporating a mathematical modeling of continuous media, discontinuity, cracks and particle mechanisms in a single structure [3]. However, to make the PD capable of better representing heterogeneous materials we have to change the way with G_f is spatially distributed in the model. The random field used in this work was implemented within the PD context by Friedrich et al. [4], however the goal now is to extend

this first study to a detailed analysis of the parameters that influence the random field and how it will help in the modeling of heterogeneous materials with PD.

2 Bond-Based Peridynamics

Peridynamics is a nonlocal theory of continuum media able to eliminate the mathematical inconsistency present in the classical continuum media theory by substituting the spatial derivatives by force integrals in the material points in the spatial domain. The PD theory divides a continuum media into material points occupying volume in space, Fig. 1. The most important point of the PD formulation is that each material point has its behavior governed by the interaction with the points located in its neighborhood. In other words, the PD theory is about the interaction forces between material points within a given neighborhood [5].

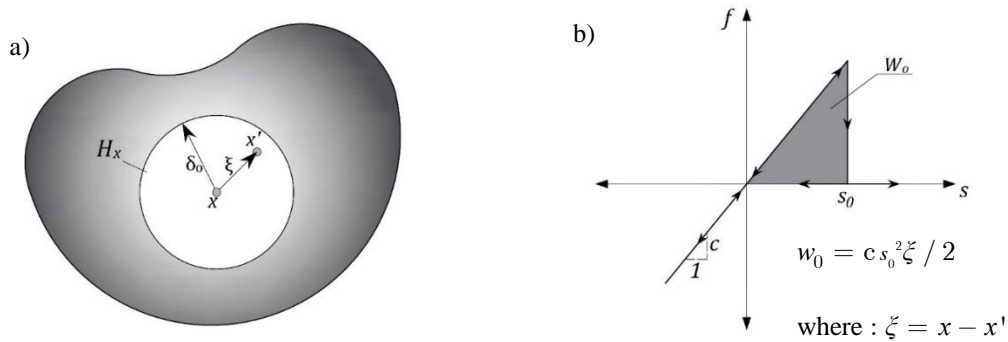


Figure 1. a) A scheme with the main parameters used in the PD [6], b) The uniaxial constitutive law to simulate damage [7]

There are many PD formulations since its creation; however, the bond-based theory [6] satisfies the requirements for the aim of this work, despite its limitations, and results in a computational advantage because of its simple application. The term “bond” refers to the interaction between the material points at x and x' . The Eq. (1) presents the bond-based PD equation of motion,

$$\rho(x)\ddot{u}(x, t) = \int_{H_x} f(u' - u, x' - x) dV' + b(x, t) \quad (1)$$

where ρ is the material density, $b(x, t)$ is the body force acting at point x and H_x is the space of the material points near the point x , Fig. 1a. $f(u' - u, x' - x)$ is a pairwise force density vector function and u is the displacement of the material point at x ; f contains all the constitutive properties of the material and for a linear elastic isotropic solid, for instance, can be expressed as Eq. (2).

$$f(u' - u, x' - x) = cs \frac{y' - y}{|y' - y|} \quad (2)$$

where $y = x + u$ is the position of the material point in the deformed configuration. The bond constant c is the peridynamic material parameter and can be expressed in terms of the material constants of Classic continuum mechanics (Javili *et al.* 2018). That is, for a linear isotropic material, the bond constant is given by:

$$c = 12E/\pi\delta_0^4 \quad (3)$$

where E is the elastic modulus of material. In the Eq. (2), s is the bond stretch expressed on the following form,

$$s = \frac{|y' - y| - |x' - x|}{|x' - x|} \quad (4)$$

In the PD model damage is introduced by means of bond breaking. The bonds lose their load capacity when

a limit s_0 is reached, as it is shown in Fig. 1b. w_0 is the work required to break an individual bond and could be represented as the area under the f - s bond law, in Fig.1b [8]. The energy per unit of fracture area required to separate the body can be expressed in the Eq. (5), for a 3D case, and thus, the critical stretch s_0 can be determined by the material fracture energy.

$$G_f = \frac{\pi c s_0 \delta^5}{10} \rightarrow s_0 = \sqrt{\frac{5G_f}{6E\delta_0}} \quad (5)$$

In order, to compute the fracturing process is applied a local characteristic function φ to identify the connection state of each bond, as follows

$$\vartheta(\eta, \xi, t) = \begin{cases} 1, & s \leq s_0 \\ 0, & s > s_0 \end{cases} \quad \text{and} \quad \varphi = 1 - \frac{\int_{H_x} \vartheta dV_\xi}{\int_{H_x} dV_\xi} \quad (6)$$

Therefore, if a particle has no broken bonds its local damage is $\varphi = 0$, on the other hand if the point is completely disconnected from the rest of the body its value is $\varphi = 1$.

2.1 3D Random Field Generation

In the work carried out by Friedrich et al. [4] a methodology was presented to generate a random toughness field regardless of discretization used in the PD model. The methodology was originally proposed by Miguel *et al.* [9] and more recently implemented in a version of Discrete Element Method (DEM) by Puglia *et al.* [10]. The random properties are equally distributed along the correlation length (l_{cor}). The approach consists of dividing the domain formed by the material points into prismatic regions that have their sides formed by the correlation lengths, which can be different in the three Cartesian directions (l_{cx} , l_{cy} , l_{cz}), see Fig. 2. The line of axes X_G , Y_G and Z_G represents the global coordinate system used to reference the global model. Each PD bounds i of the system is referenced by a new coordinate system X_{Gi} , Y_{Gi} and Z_{Gi} , and by the local coordinate system within the prism x_i , y_i and z_i .

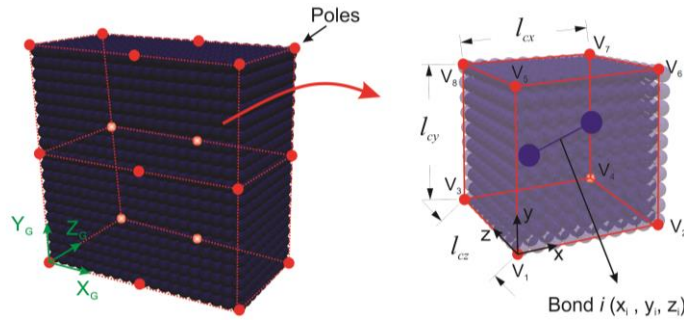


Figure 2. Vertices location and the correlation length in the domain of the PD model

At each vertices of these prisms ($V_1 \dots V_8$) are assigned random values with uncorrelated probabilities distributions. Subsequently, to determine the value of the random field corresponding to each bond i inside the prism a three-dimensional (3D) interpolation is performed. In the present implementation, the spatial localization of the PD bonds i is characterized by the coordinates of its barycenter (x_i , y_i , z_i). The 3D interpolation is given as follow,

$$\begin{aligned} \varphi_v(x_i, y_i, z_i) = & V_1 + \frac{V_2 + V_1}{l_{cx}} x_i + \frac{V_3 - V_1}{l_{cy}} y_i + \frac{V_5 - V_1}{l_{cz}} z_i + \frac{V_4 - V_3 - V_2 + V_1}{l_{cx} l_{cy}} x_i y_i + \\ & \frac{V_6 - V_5 - V_3 + V_1}{l_{cx} l_{cz}} x_i z_i + \frac{V_7 - V_5 - V_3 + V_1}{l_{cy} l_{cz}} y_i z_i + \frac{V_8 - V_7 - V_6 + V_5 - V_4 + V_3 + V_2 - V_1}{l_{cx} l_{cy} l_{cz}} x_i y_i z_i \end{aligned} \quad (7)$$

where $\varphi_v(x_i, y_i, z_i)$ is the interpolated random value for bond i of coordinates x_i, y_i, z_i . V_k ($k = 1, 2, 3, \dots, 8$) is the values of the random field at the vertices. The randomness of the material properties in V_k considers that the G_f is a random field with a distribution of Type III (Weibull), characterized by Eq. (8).

$$F(G_f) = 1 - \exp[-(G_f / \beta)^\gamma] \quad (8)$$

where β and γ are the scaling and shape parameters, respectively. The mean μ and the standard deviation sd are related to the scale and shape parameters by means of the Eq. (9).

$$\mu = \beta(\Gamma(1 + 1 / \gamma)) \quad sd = \beta[\Gamma(1 + 2 / \gamma) - \Gamma^2(1 + 1 / \gamma)]^{1/2} \quad (9)$$

where Γ is the Gamma function. Since G_f and s_0 are directly related (Eq. (5)), it is possible to prove that approximately $CV_{s_0} = 0.5 CV_{G_f}$, see Hahn and Shapiro [11].

3 Model description

To analyze the behavior of the generated random field, was used a PMMA plate as PD model, with the dimensions shown in Figure 3. The Figure 3 also details the boundary conditions regions and the mechanical properties of the material used. The plates are subjected to a uniaxial tensile test, fixing the lower part and applying a prescribed displacement in the upper region. The thickness of the plate is set at $3.015dx$, where dx is the distance between each material point, which defines the model's discretization. The δ_0 horizon also depends on the distance from each material point, making the horizon a parameter of the simulation, where $\delta_0 = 3.015dx$. In order to better analyze what occurs in the xy plane of the plate, in all cases lc_z was defined as 0.2 m, that is, a value quite distant from the other poles so that it does not influence the response

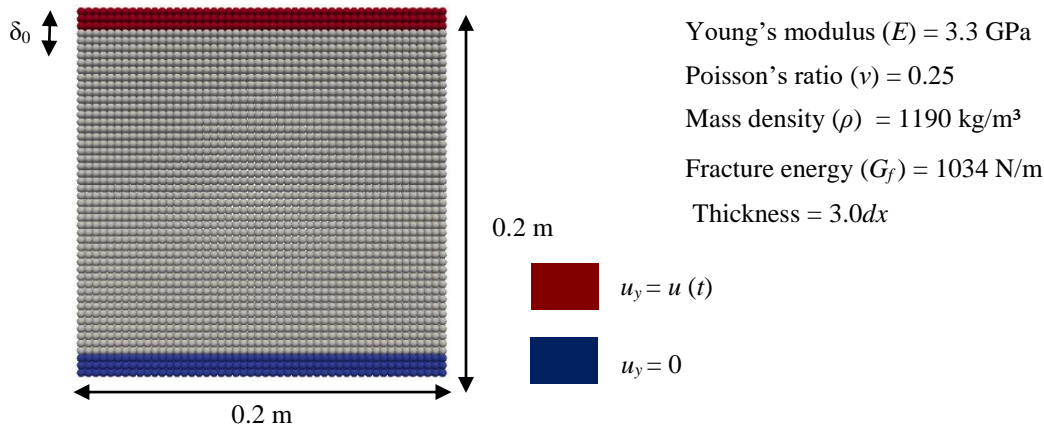


Figure 3. Plate dimensions and boundary conditions applied

With the methodology previously described in Section 2, was generated a value of G_f for each pole. From these G_f values, was obtained the critical stretching (s_0), for each pole too. Thus, the 3D interpolation for each bond (Eq. 7) of the PD model can be determined. Randomness is introduced in the model through a mean value of G_f and a standard deviation (s_d). The relation between these two parameters can be introduced through a coefficient of variation (CV_{G_f}). In the next section, a parametric study of the influence of correlation length (lc_{or}), CV_{G_f} and discretization (dx) will be presented.

4 Results and discussion

To illustrate the importance of the correlated random field in the mechanical properties of the material, an uncorrelated (Fig. 4a) and correlated (Fig. 4b) with $lc_x, y = 0.02$ m is compared in Fig. 4. Consider the plate shown in Fig. 3 with $dx = 0.004$ m and $CV_{G_f} = 50\%$. The color map represents the distribution of G_f in the middle plane of the thickness in $1.5dx$. It is clear that the correlation length decreases the fluctuation of G_f values for the same

point (width), making the toughness distribution more correct within the PD model.

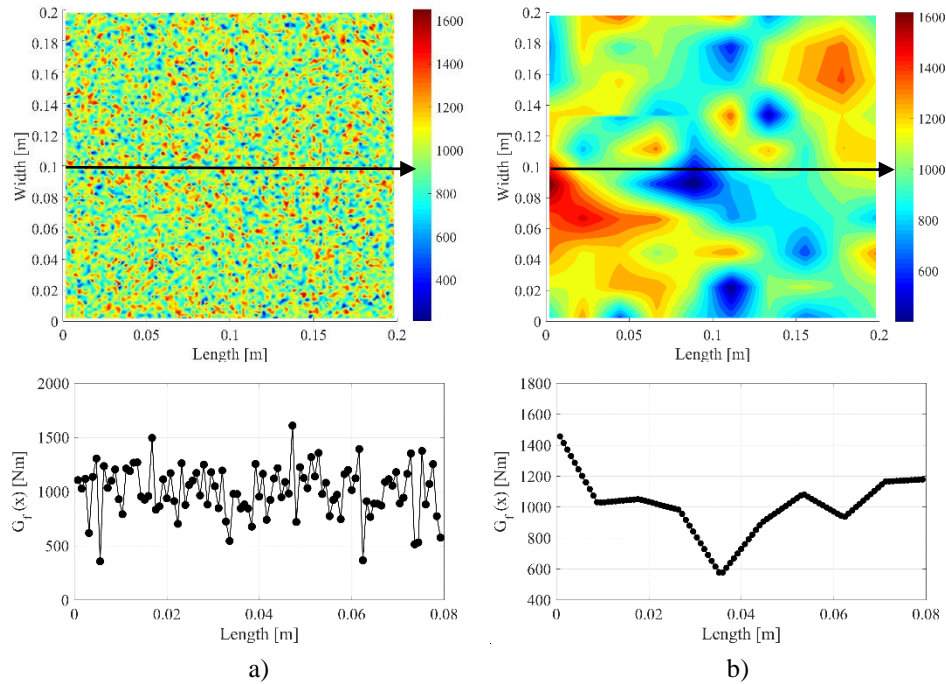


Figure 4. G_f random field with: a) uncorrelated and, b) correlated with $lc_{x,y} = 0.02$ m

Figure 5 shows the influence of different coefficients of variation of CV_{G_f} , for the plate configurations of Figure 4. Figure 5a shows the spatial distribution of G_f that remains the same for all cases, however, as CV_{G_f} increases or decreases the points weaker (in blue) or stronger (red) are highlighted. Figure 5b shows the behavior of the Load vs. Displacement curves for the analyzed cases. It is observed that the CV completely changes the loading curves because the weakest points highlighted in the random field make the plate more susceptible to fail more quickly. Therefore, CV_{G_f} can also be used as an adjustment parameter in the peridynamic simulation in search of better results.

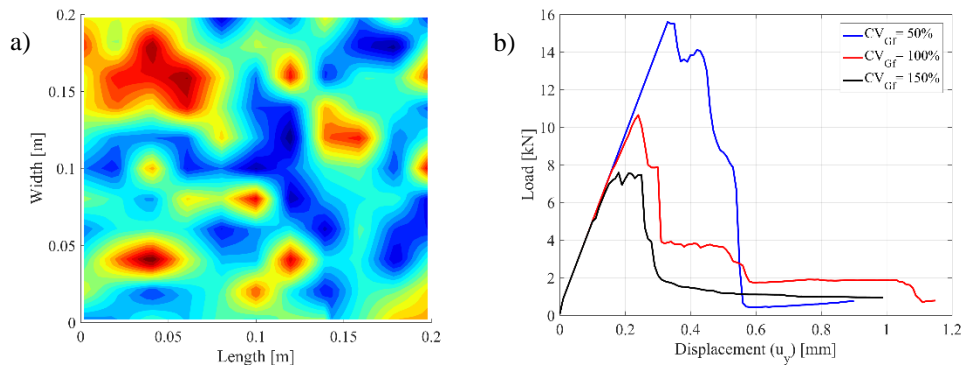


Figure 5. a) G_f random field and, b) Load vs. Displacement for different CV_{G_f}

Figure 6 shows the final rupture configuration for the cases shown in Fig. 5. It is important to note that, as the CV_{G_f} increases, the crack path changes through the "weakest" region. Therefore, propagation occurs with two competitive tendencies in the PD model: the stress level in the plate and the percentage of G_f variation, CV_{G_f} .

To evaluate the independence of the rupture configuration for the model discretization, three levels of discretization were analyzed, $dx = 0.025$ (8x8 points), 0.0025 (80x80 points) and 0.00125 (160x160 points). A

correlation length of $lc_x, y = 0.02$ m and $CV_{G_f} = 50\%$ was considered for all cases.

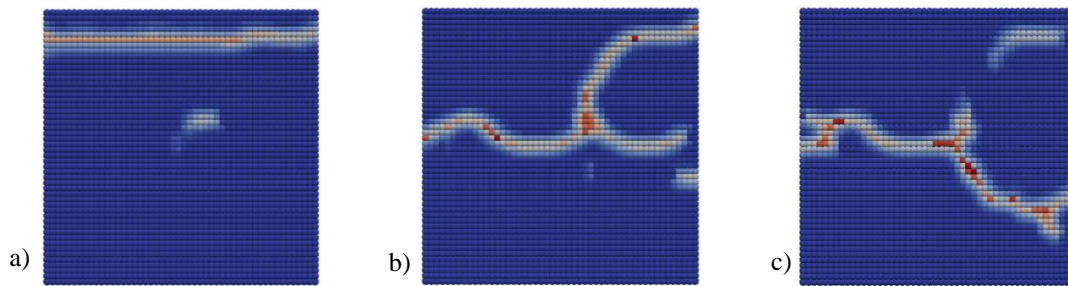


Figure 6. Final rupture configuration for different CV_{G_f} : a) 50%, b) 100% and, c) 150%

Figure 7 shows the distribution of G_f for the three discretizations adopted together with the final rupture configuration of each case. Analyzing the figures we can see that the random fields have the same configuration but have different intensities, this is due to the interference of the number of connections. In the boards with the least amount of connections, that is, with large dx , as shown in Fig. 7a, the peaks of higher and lower values do not affect significantly. In the plates where the number of material points becomes greater (small dx), the cracks propagate in a more defined way, with the field accentuating its weakest points.

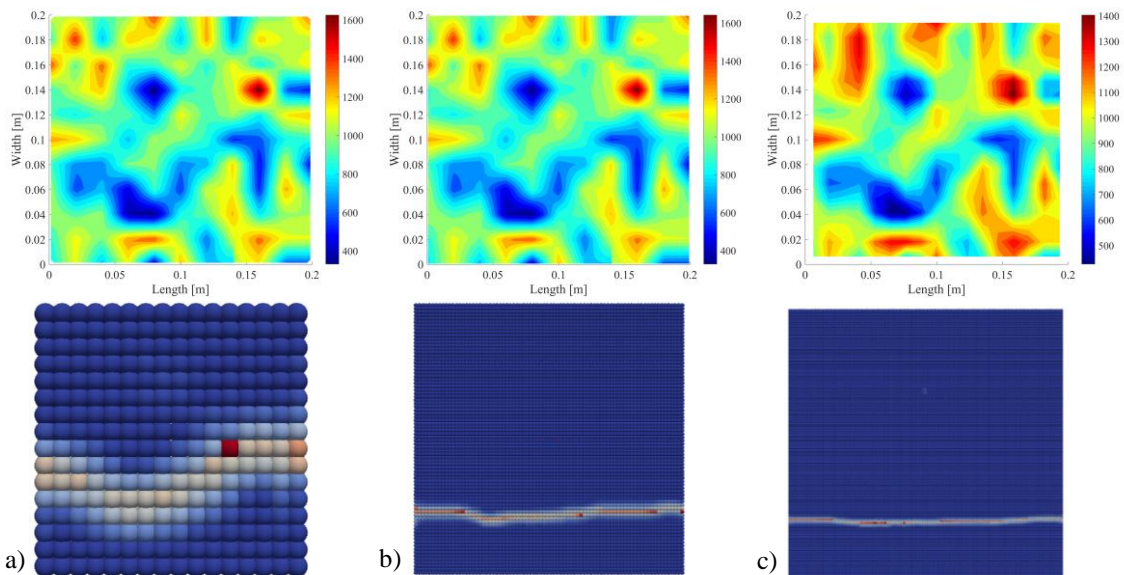


Figure 7. G_f random field and final rupture configuration for: a) $dx = 0.025$ m, b) $dx = 0.0025$ m and, c) $dx = 0.00125$ m.

It is important to remember that the random values of G_f are applied to the poles and do not represent the value passed on to the PD model. To measure the influence of the G_f variation within the PD model, it is necessary to analyze what happens in the family (H_x) of each material point, since this is really the control volume of interest. The plate in the previous case, however, with $lc_x = lc_y = lc_z = 3dx$, was analyzed for different values of CV_{G_f} and the mean CV of the families at each point, called CV_{H_x} , was analyzed. Figure 8a shows that the relation between CV_{G_f} and CV_{H_x} is approximately 4 times for more usual variations, that is, less than 200%. From the presented relationship it is also possible to create a quadratic adjustment curve between the coefficients to predict a desired real variation of G_f within the model.

Figure 8b shows the influence of the correlation length, and the coefficient of variation within the control volume, CV_{H_x} , considering $CV_{G_f} = 50\%$. In the x and y directions, lc_x and lc_y are equal and lc_z has been put away from the xy plane again. They were analyzed in 6 different correlation lengths, representing from a more

homogeneous material, with a longer correlation length, to a completely disordered material with $l_{cor} = l_x = l_y = 0.0013$ m. Fig. 8b shows that a difference of approximately 9% in the CV_{Hx} is achieved, which represents a significant influence that certainly affects the global behavior of the material. However, when l_{cor} is small, this difference is not significant, assuming that at this point there is a complete uncorrelation of properties.

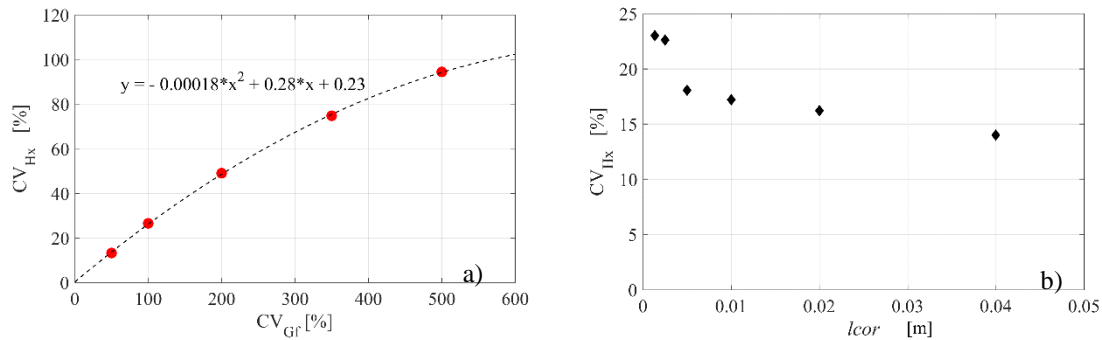


Figure 8. a) Relation between CV_{Gf} and CV_{Hx} , and b) influence of the correlation length l_{cor}

5 Conclusions

The parametric study showed how the parameters change the behavior of the material and the ability of the PD to expand its application in the field of heterogeneous materials. CV_{Gf} has a strong influence on the crack path, while l_{cor} governs the level of heterogeneity that one wants to model. These two parameters served to help calibrate the PD model and better adapt to the final rupture configurations recorded in experimental tests.

Acknowledgements. The authors thank the Coordenação de Aperfeiçoamento de Pessoal de Nível Superior - Brasil (CAPES), the National Council for Scientific and Technological Development (CNPq) and FAPERGS, research support foundation of the RS state for the financial support for research in Brazil.

Authorship statement. The authors hereby confirm that they are the sole liable persons responsible for the authorship of this work, and that all material that has been herein included as part of the present paper is either the property (and authorship) of the authors, or has the permission of the owners to be included here.

References

- [1] S. Torquato, *Random Heterogeneous Materials: Microstructure and Macroscopic Properties*, Springer, 2013.
- [2] X. Liu and V. Shapiro, “Random heterogeneous materials via texture synthesis”, *Computational Materials Science*, vol. 99, pp. 177-189, 2015.
- [3] A.S. Fallah, I.N. Giannakeas, R. Mella et al., “On the Computational Derivation of Bond-Based Peridynamic Stress Tensor”, *Journal of Peridynamics and Nonlocal Modeling*, 2020.
- [4] L. Friedrich, M. Barcellos and I. Iturrioz, “Random field generation of the material properties in a peridynamic model”, In: *25th ABCM International Congress of Mechanical Engineering*, Uberlândia, MG, Brazil, 2019.
- [5] A. Javili, R. Morasata, E. Oterkusb and S. Oterkus, “Peridynamics Review”. *Mathematics and Mechanics of Solids*, 2018.
- [6] S. A. Silling and E. Askari, “A meshfree method based on the peridynamic model of solid mechanics”. *Computers & Structures*, vol. 83, pp. 1526–35, 2015.
- [7] S.A. Silling, “Reformulation of elasticity theory for discontinuities and long-range forces”. *Journal of the Mechanics and Physics of Solids*, vol. 48, pp. 175–209, 2000.
- [8] E. Madenci, E. Oterkus, *Peridynamic theory and its applications*. Springer, New York, 2014.
- [9] L.F.F. Miguel, M.L.F. Fadel, J.Jr. Kaminski, J.D. Riera and R.C.R. Menezes, “Model uncertainty in the assessment of PES wind loads in transmission line design”. *Proceedings of the International Seminar on Modeling and Identification of Structures Subject to Dynamic Excitation – emphasis of Transmission Lines*, Bento Gonçalves, Brasil, 2009.
- [10] V. B. Puglia, L. E. Kostaski, J. D. Riera and I. Iturrioz, “Random field generation of the material properties in the lattice discrete element method”. *The Journal of Strain Analysis for Engineering Design*, vol. 54, pp. 236–246, 2019.
- [11] G. J. Hahn, and S. S. Shapiro, *Statistical Models in Engineering*. John Wiley and Sons, 1967.